

# Influence of vibrational excitation on surface diffuseness of the internuclear potential: Study through heavy-ion quasielastic scattering at deep sub-barrier energies

Gurpreet Kaur,<sup>1,\*</sup> B. R. Behera,<sup>1</sup> A. Jhingan,<sup>2</sup> P. Sugathan,<sup>2</sup> and K. Hagino<sup>3,4,5</sup>

<sup>1</sup>*Department of Physics, Panjab University, Chandigarh 160014, India*

<sup>2</sup>*Inter University Accelerator Centre, Aruna Asaf Ali Marg, New Delhi 110067, India*

<sup>3</sup>*Department of Physics, Tohoku University, Sendai 980-8578, Japan*

<sup>4</sup>*Research Center for Electron Photon Science, Tohoku University, 1-2-1 Mikamine, Sendai 982-0826, Japan*

<sup>5</sup>*National Astronomical Observatory of Japan, 2-21-1 Osawa, Mitaka, Tokyo 181-8588, Japan*

(Received 18 August 2015; published 15 October 2015)

We discuss the role of channel coupling in the surface properties of an internuclear potential for heavy-ion reactions. To this end, we analyze the experimental quasielastic cross sections for the  $^{12}\text{C} + ^{105,106}\text{Pd}$  and  $^{13}\text{C} + ^{105,106}\text{Pd}$  systems using the coupled-channels approach by including the vibrational excitations in the target nuclei. While earlier studies have reported a negligible influence of vibrational excitation on the surface diffuseness parameter for spherical systems, we find a significant effect for the C + Pd systems. Our systematic study also reveals influence of transfer couplings on the surface diffuseness parameter.

DOI: [10.1103/PhysRevC.92.044609](https://doi.org/10.1103/PhysRevC.92.044609)

PACS number(s): 25.70.Bc, 24.10.Eq, 25.70.Hi

## I. INTRODUCTION

Even though fusion cross sections reflect the dynamical behavior of the nuclei involved in the fusion [1], apparently it is not possible to get insights into the interaction mechanism between nuclei simply by measuring fusion cross sections. That is, theoretical calculations, such as coupled-channels calculations (either semiclassical or quantal), are indispensable in order to understand the fusion dynamics [2–5]. These calculations, in comparison with the experimental data, address the influence of coupling between the relative motion and the nuclear intrinsic degrees of freedom, and thus the interplay between nuclear structure and reaction dynamics [6,7]. As a result, the coupled-channels formalism has become a powerful and standard tool in order to interpret experimental fusion cross sections [4].

One of the most important ingredients of such calculations is an internuclear potential. Various types of potential, such as a double folding potential [8,9] and a phenomenological Woods-Saxon potential [10], have been employed. Among these, the Woods-Saxon form, described by the depth parameter,  $V_0$ , the radius parameter,  $r_0$ , and the surface diffuseness parameter,  $a_0$ , has gained popularity due to its simplicity and ability to reproduce many experimental results. While representing the Woods-Saxon potential, its depth and radius parameters can be mutually adjusted to reproduce the Coulomb barrier of the system once the surface diffuseness parameter is fixed. Obtaining the quantitative measure for the surface diffuseness parameter is therefore of crucial importance, as the curvature of the Coulomb barrier is largely determined by the surface diffuseness parameter, which by definition reflects the surface property of the internuclear potential.

Three different methods have been used in literature in order to extract a diffuseness parameter from experimentally measured data. The first method is to analyze elastic scattering

cross sections either with an optical potential model or with a coupled-channels approach. This method has established a value of surface diffuseness to be around 0.6 fm for most of the systems [11]. The second method is to use high-precision fusion cross section. It has turned out that this method leads to a much larger value of surface diffuseness parameter, ranging from 0.75 to 1.5 fm, than the first method [12,13]. Recently, Hagino *et al.* have proposed a third method, which uses a quasielastic (QE) excitation function at large backward angles [14]. They have suggested that, at energies well below the Coulomb barrier, a QE excitation function is sensitive mainly to the surface property of nuclear potential and can be used to obtain quantitatively the surface diffuseness parameter. This method leads to the diffuseness parameter for spherical systems being around 0.6 fm [15], while somewhat larger values of the diffuseness parameter have been obtained for systems involving deformed nuclei.

The different values of surface diffuseness parameter, obtained for spherical and deformed systems, lead to a realization that not only obtaining the quantitative measure of diffuseness but also understanding how the coupling affects the surface diffuseness is of importance. For this purpose, several studies have been carried out, aiming to understand the effects of different couplings on the surface diffuseness parameter. Gasques *et al.* [17] have performed both the single-channel (sc) and the coupled-channels (cc) calculations for  $^{32}\text{S} + ^{208}\text{Pb}$ ,  $^{197}\text{Au}$ ,  $^{186}\text{W}$ , and  $^{170}\text{Eu}$  systems and concluded that the rotation coupling shows a significant influence on the diffuseness parameter value. See also Ref. [18]. Washiyama *et al.* [15] have analyzed the QE measurements for  $^{16}\text{O}$  and  $^{32,34}\text{S} + ^{208}\text{Pb}$  systems with the single-channel calculations. They did not obtain any enhancement in the value of surface diffuseness parameter, and thus a significant effect of vibrational coupling on the diffuseness parameter was not observed. Studies on many other systems, such as  $^{16,17,18}\text{O} + ^{92}\text{Mo}$  [16], have also shown similar results. Hence, it has generally been considered that the vibrational excitation has a marginal effect on the surface diffuseness parameter.

\*gkaur.phy@gmail.com

The aim of this paper is to investigate further the effect of vibrational excitations on the surface diffuseness parameter. As in the rotational excitations, one may expect that the effect becomes more significant when the vibrational excitation energy is small. Furthermore, we also investigate the effect of transfer coupling, which has been established to play an important role in the fusion dynamics [19]. To the best of our knowledge, no study has reported how the transfer coupling affects the diffuseness parameter. For these purposes, we reanalyze the experimental data for  $^{12,13}\text{C} + ^{105,106}\text{Pd}$  systems reported in Ref. [20] using the coupled-channels approach.

The paper is organized as follows. In Sec. II, we first discuss the characteristic feature of the  $^{12,13}\text{C} + ^{105,106}\text{Pd}$  systems with respect to the vibrational and the transfer couplings. We then detail the procedure to extract the surface diffuseness parameter through the analyses of the quasielastic data. In Sec. III, we present the results of our analyses and discuss the role of vibrational and transfer couplings. Finally, we summarize the paper in Sec. IV.

## II. METHOD

### A. Systems

In order to study the effect of vibrational coupling on a surface diffuseness parameter, we reanalyze the experimental quasielastic scattering for the  $^{12,13}\text{C} + ^{106,106}\text{Pd}$  systems, for which the data have been available in Ref. [20]. While Ref. [20] focused on extracting the barrier distributions, our aim in this paper is to extract the surface diffuseness parameter using the deep-sub-barrier data. We choose these systems as the target nuclei,  $^{105,106}\text{Pd}$ , exhibit low-energy vibrational excitations ( $E^* \approx 0.5$  MeV for the first excited state in  $^{104,106}\text{Pd}$ ). The projectile,  $^{13}\text{C}$ , along with the chosen target, is an ideal candidate to study the effect of transfer coupling due to the following characteristics:

- (i) Positive  $Q$  values for one-neutron transfer channels (see Table I), which are necessary for a system to exhibit significant influences of a neutron transfer coupling [19,21].
- (ii) The existence of the weakly bound valence nucleon, which ensures the transfer of neutron.
- (iii) Vibrational couplings in the target nuclei, which are in general weaker as compared to rotational couplings so that the effect of transfer may not be significantly masked.

TABLE I. The  $Q$  value for the neutron transfer channels for the  $^{12,13}\text{C} + ^{105,106}\text{Pd}$  systems, given in units of MeV. Here the negative and positive signs correspond to the pickup and stripping reactions, respectively.

System	$(-1n)$	$(-2n)$	$(+1n)$	$(+2n)$
$^{12}\text{C} + ^{105}\text{Pd}$	-9.161	-15.744	-2.148	-3.953
$^{12}\text{C} + ^{106}\text{Pd}$	-12.185	-16.082	-4.615	-3.532
$^{13}\text{C} + ^{105}\text{Pd}$	+4.615	-7.571	+1.082	-7.681
$^{13}\text{C} + ^{106}\text{Pd}$	+1.59	-7.908	-1.385	-7.261

In our systematic study, we carry out the coupled-channels calculations by including the vibrational couplings in the target nuclei in order to understand the influence of the vibrational coupling on the surface diffuseness parameter. Moreover, since the  $^{12}\text{C} + ^{105,106}\text{Pd}$  systems have a negative  $Q$  value for the neutron pickup reactions (see Table I), a comparison with the  $^{13}\text{C} + ^{105,106}\text{Pd}$  systems will elucidate the role of transfer coupling in the surface diffuseness parameter.

### B. Procedure

To perform a systematic study, the single-channel and coupled-channel calculations have been performed using a scattering version of the CCFULL program [22]. For the coupled-channels calculations, we have included the double quadrupole phonon excitations in the target nuclei in the harmonic oscillator limit. The deformation parameter and the excitation energy for  $^{106}\text{Pd}$  are given by  $\beta = 0.229$  and  $E^* = 0.512$  MeV, respectively [20]. For the  $^{105}\text{Pd}$  nucleus, we have followed Ref. [20] and have taken the average in the adjacent nuclei, that is,  $^{104}\text{Pd}$  and  $^{106}\text{Pd}$ , which leads to  $\beta = 0.219$  and  $E^* = 0.534$  MeV.

The nuclear potential used in the calculations has real and imaginary components, both of which are assumed to have a Woods-Saxon form. The imaginary part simulates a compound nucleus formation. We have chosen the strength to be large enough so that the flux does not reflect inside the barrier once the barrier is overcome. In the calculations, we have used an imaginary potential with the depth parameter of 30 MeV, a radius parameter of 1.0 fm, and a diffuseness parameter of 0.3 fm. This choice of parameters confines the imaginary potential well inside the Coulomb barrier with a negligible strength in the surface region. As long as the imaginary potential is confined inside the Coulomb barrier with a large strength, the results are insensitive to the parameters of the imaginary part. For the real part of the nuclear potential, the potential depth  $V_0$  is fixed to be 185 MeV. The value of radius parameter  $r_0$  is then adjusted for a particular value of the diffuseness parameter such that the Coulomb barrier height  $V_B$  for each system becomes the same as that for the Bass potential [23]. This is possible because the effect of variation in  $V_0$  and  $r_0$  on the Coulomb barrier height compensates with each other in the surface region. That is, for a given value of diffuseness parameter, the results do not significantly depend upon the actual choice of  $V_0$ , as long as the same barrier height  $V_B$  is maintained.

To ensure that the barrier height for the single-channel and the coupled-channels calculations corresponds to the same value, we have slightly readjusted the potential parameters for the coupled-channels calculations by using the fusion cross sections at energies above the barrier. The following steps have been taken for this purpose:

- (i) For a chosen and fixed value of the diffuseness parameter  $a_0$ , and with the depth  $V_0 = 185$  MeV, the value of the radius parameter  $r_0$  is determined such that the Coulomb barrier energy  $V_B$  reproduces the Bass barrier.

- (ii) The fusion cross sections,  $\sigma_{\text{fus}}^{(sc)}$ , are calculated using the single-channel calculation.
- (iii) The full coupled-channels calculations are then performed to obtain the fusion cross sections in the presence of the channel couplings,  $\sigma_{\text{fus}}^{(cc)}$ . In general, even at energies above the barrier, these fusion cross sections are different from  $\sigma_{\text{fus}}^{(sc)}$  due to the potential renormalization [24]. By slightly adjusting the radius parameter,  $r_0$ , we match the fusion cross sections  $\sigma_{\text{fus}}^{(cc)}$  at energies well above the barrier with  $\sigma_{\text{fus}}^{(sc)}$ . This results in a set of potential parameters ( $V_0$ ,  $r_0$ ,  $a_0$ ) that reproduces the fusion barrier height by taking into account the couplings to the intrinsic states with the coupled-channels calculations.
- (iv) For every set of nuclear potential parameters, both for the single-channel and the coupled-channels analyses, the quasielastic scattering cross sections are computed. For the single-channel calculation, the quasielastic cross section corresponds simply to the elastic scattering cross section. On the other hand, for the coupled-channels calculations, the quasielastic cross sections correspond to a sum of elastic and inelastic cross sections.

In order to find the best-fitted value of the diffuseness parameter, the  $\chi^2$  method has been utilized. To this end, the data with  $d\sigma_{\text{qel}}/d\sigma_{\text{R}} > 1$ , where  $d\sigma_{\text{qel}}/d\Omega$  and  $d\sigma_{\text{R}}/d\Omega$  are quasielastic and the Rutherford cross sections, respectively, have been excluded from the fitting procedures, even though they are included in the figures for completeness. The uncertainty in the optimum value of  $a_0$  has been calculated using the following procedure. For the  $\chi_{\text{min}}^2$  value corresponding to the best-fit value of the diffuseness parameter, the quantity  $(\chi_{\text{min}}^2 + \chi_{\text{min}}^2/n)$  was calculated, where  $n$  denotes the number of degrees of freedom. The intersection of this quantity with the  $\chi^2$  envelope gives the two values  $a_0^-$  and  $a_0^+$  defining the error in  $a_0$ .

For the  $^{12}\text{C} + ^{105,106}\text{Pd}$  and  $^{13}\text{C} + ^{105,106}\text{Pd}$  systems, the QE excitation functions have been measured at  $165^\circ$  in the laboratory frame as reported in Ref. [20]. To be consistent, all the calculations have been carried out at the same scattering angle. In order to ensure that the calculations are properly scaled according to the available data, the calculated ratio of the quasielastic to the Rutherford cross sections are analyzed and plotted as functions of the effective energy defined as [25,26]

$$E_{\text{eff}} = \frac{2E_{\text{c.m.}}}{1 + \text{cosec}\left(\frac{\theta_{\text{c.m.}}}{2}\right)}, \quad (1)$$

where  $E_{\text{c.m.}}$  and  $\theta_{\text{c.m.}}$  are energy and scattering angle in the center-of-mass frame, respectively. This corrects for the angle-dependent centrifugal effects by making  $\sigma_{\text{qe}}(E_{\text{eff}}, 180^\circ) \approx \sigma_{\text{qe}}(E_{\text{c.m.}}, \theta_{\text{c.m.}})$ .

### III. RESULTS AND DISCUSSION

#### A. Single-channel calculations

Let us now numerically extract the surface diffuseness parameter from the experimental data for the quasielastic

TABLE II. The optimum value of the surface diffuseness parameter,  $a_0$ , obtained with the single-channel and the coupled-channels calculations. Those values are given in units of fm.

System	Single channel	Coupled channels
$^{12}\text{C} + ^{105}\text{Pd}$	$0.80 \pm 0.04$	$0.69 \pm 0.04$
$^{12}\text{C} + ^{106}\text{Pd}$	$0.94 \pm 0.07$	$0.78 \pm 0.05$
$^{13}\text{C} + ^{105}\text{Pd}$	$0.64 \pm 0.05$	$0.60 \pm 0.05$
$^{13}\text{C} + ^{106}\text{Pd}$	$0.76 \pm 0.04$	$0.68 \pm 0.03$

scattering. We have first performed the single-channel calculations without including the inelastic excitations of the target nuclei. The value of  $a_0$  has been extracted using the procedure explained in the previous section. After the  $\chi^2$  fitting, the best-fitted value of  $a_0$  for the  $^{12}\text{C} + ^{105}\text{Pd}$  and  $^{12}\text{C} + ^{106}\text{Pd}$  systems have been found to be  $0.80 \pm 0.04$  fm and  $0.94 \pm 0.07$  fm, respectively. The quasielastic cross sections obtained with several values of the surface diffuseness parameter are shown in Figs. 1(a) and 1(b) for the  $^{12}\text{C} + ^{105}\text{Pd}$  and  $^{12}\text{C} + ^{106}\text{Pd}$  systems, respectively. The  $\chi^2$  fit for the  $^{12}\text{C} + ^{105}\text{Pd}$  system is shown in Fig. 2. Similarly, for the  $^{13}\text{C} + ^{105}\text{Pd}$  [shown in Fig. 1(c)] and  $^{13}\text{C} + ^{106}\text{Pd}$  systems [shown in Fig. 1(d)], the best-fitted values of  $a_0$  after minimizing the  $\chi^2$  have been found to be  $0.64 \pm 0.05$  fm and  $0.76 \pm 0.04$  fm, respectively.

The optimum values of the surface diffuseness parameter are summarized in Table II. We notice that these values are significantly larger than the standard value of around 0.6 fm (obtained from elastic scattering cross sections), which are in a similar situation as in systems with a deformed target.

#### B. Coupled-channels calculations

In order to investigate whether the large values of surface diffuseness parameter obtained with the single-channel calculations are due to the neglect of channel coupling effects, we have next performed the coupled-channels calculations including the vibrational excitations in the target nuclei,  $^{105,106}\text{Pd}$ . The value of  $a_0$  has been varied and the best-fitted value has been obtained after the  $\chi^2$  minimization. The comparison of the coupled-channels calculations with several values of  $a_0$  with the experimental data is shown in Fig. 3. The best fitted value of  $a_0$  for the  $^{12}\text{C} + ^{105}\text{Pd}$  [shown in Fig. 3(a)] and the  $^{12}\text{C} + ^{106}\text{Pd}$  systems [shown in Fig. 3(b)] have been found to be  $0.69 \pm 0.04$  fm and  $0.78 \pm 0.05$  fm, respectively. Similarly, the best-fitted value of  $a_0$  for the  $^{13}\text{C} + ^{105}\text{Pd}$  [shown in Fig. 3(c)] and the  $^{13}\text{C} + ^{106}\text{Pd}$  systems [shown in Fig. 3(d)] are  $0.60 \pm 0.05$  fm and  $0.68 \pm 0.03$  fm, respectively. Those values are summarized in Table II.

It is apparent from Table II that the diffuseness parameter decreases in the coupled-channels calculations as compared to the single-channel calculations with inert target nuclei. This observation is similar to that observed in the case of rotational coupling [17]. Notice that earlier studies with systems such as  $^{32}\text{S} + ^{208}\text{Pb}$  did not show any influence of a vibrational excitation on the diffuseness [17]. In contrast, our calculations for the  $^{12}\text{C} + ^{105,106}\text{Pd}$  and  $^{13}\text{C} + ^{105,106}\text{Pd}$

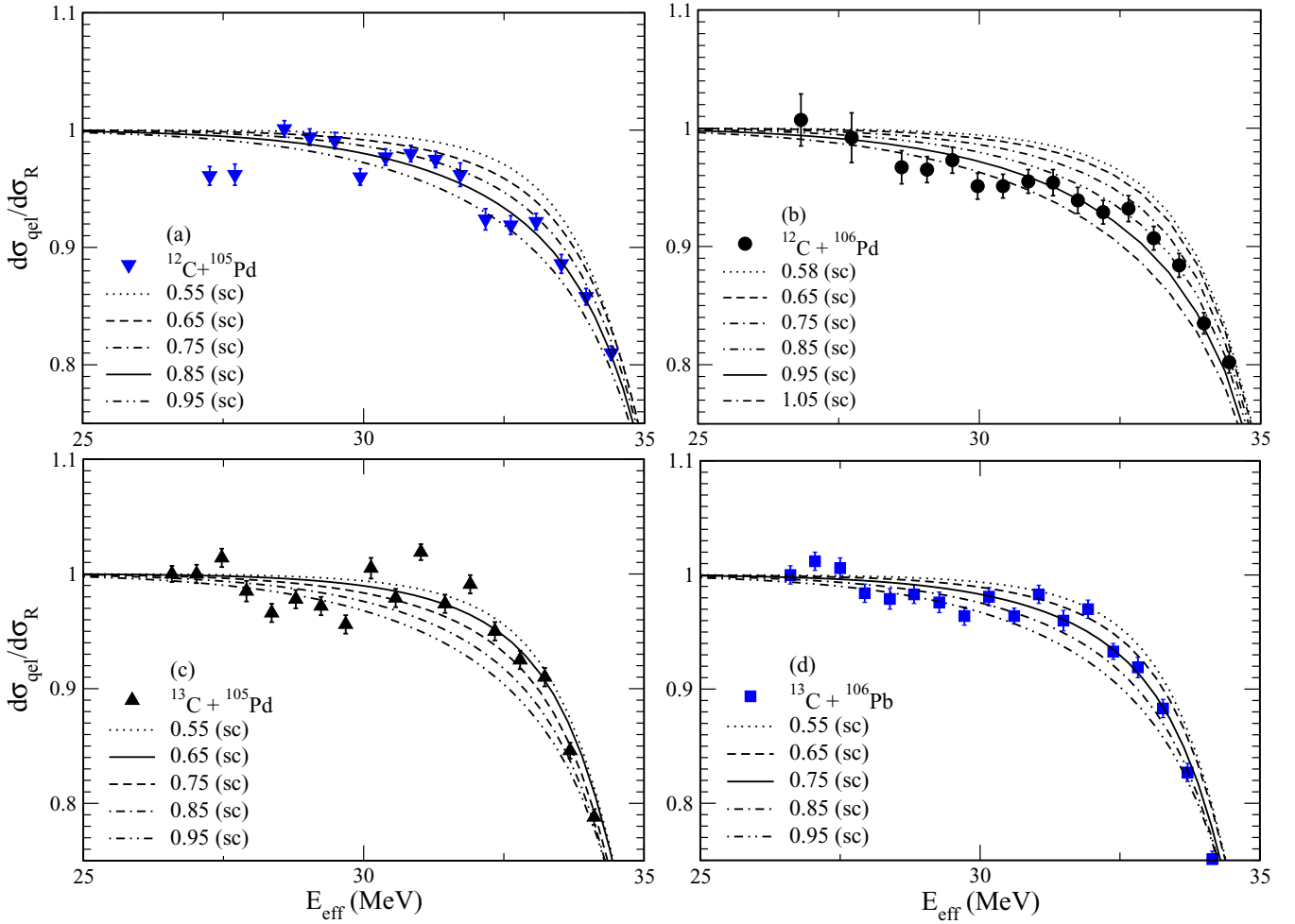


FIG. 1. (Color online) Comparisons of the single-channel calculations for the quasielastic excitation function obtained with several values of the surface diffuseness parameter,  $a_0$ , in the nuclear potential. The panels (a), (b), (c), and (d) are for the  $^{12}\text{C} + ^{105}\text{Pd}$ ,  $^{12}\text{C} + ^{106}\text{Pd}$ ,  $^{13}\text{C} + ^{105}\text{Pd}$ , and  $^{13}\text{C} + ^{106}\text{Pd}$  systems, respectively. The experimental data are taken from Ref. [20].

systems show a significant influence even though the target nuclei are spherical.

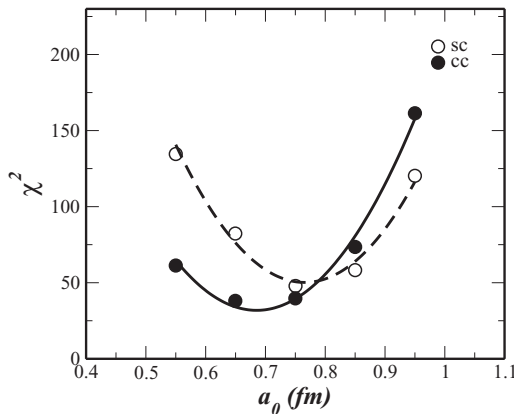


FIG. 2. The  $\chi^2$  for the  $^{13}\text{C} + ^{106}\text{Pd}$  system as a function of the surface diffuseness parameter,  $a_0$ . The open and filled symbols represent the results of the single-channel and coupled-channel calculations, respectively.

In order to understand this difference in the role of channel coupling, we proceeded to find the parameters responsible for the influence of a vibrational excitation on the surface diffuseness parameter. We have first checked whether the deformation of the nucleus is responsible for this behavior. Table III shows the deformation parameter  $\beta$  for all the spherical target nuclei,  $^{208}\text{Pb}$ ,  $^{92}\text{Mo}$ , and  $^{105,106}\text{Pd}$ . For comparison, the table also lists the deformation parameter for the deformed target nuclei,  $^{186}\text{W}$  and  $^{170}\text{Er}$  considered in Ref. [17], which are estimated from the measured  $B(E2)$  value [28] with the radius parameter of  $r_0 = 1.2$  fm. As is shown in the table,  $^{208}\text{Pb}$  and  $^{92}\text{Mo}$  have deformation parameters significantly smaller than those for deformed nuclei. For those nuclei, the vibrational effect on the surface diffuseness parameter has been found to be marginal. In contrast, the Pd isotopes have a comparably large value of  $\beta$  to the deformed nuclei, leading to a large channel coupling effect on the surface diffuseness parameter.

Naturally, one can expect that the energy of the excited state correlates with the deformation parameter. That is, as the deformation parameter is larger, the excitation energy will be smaller. Table III shows the energy of the first excited state of various nuclei considered in this paper as well as

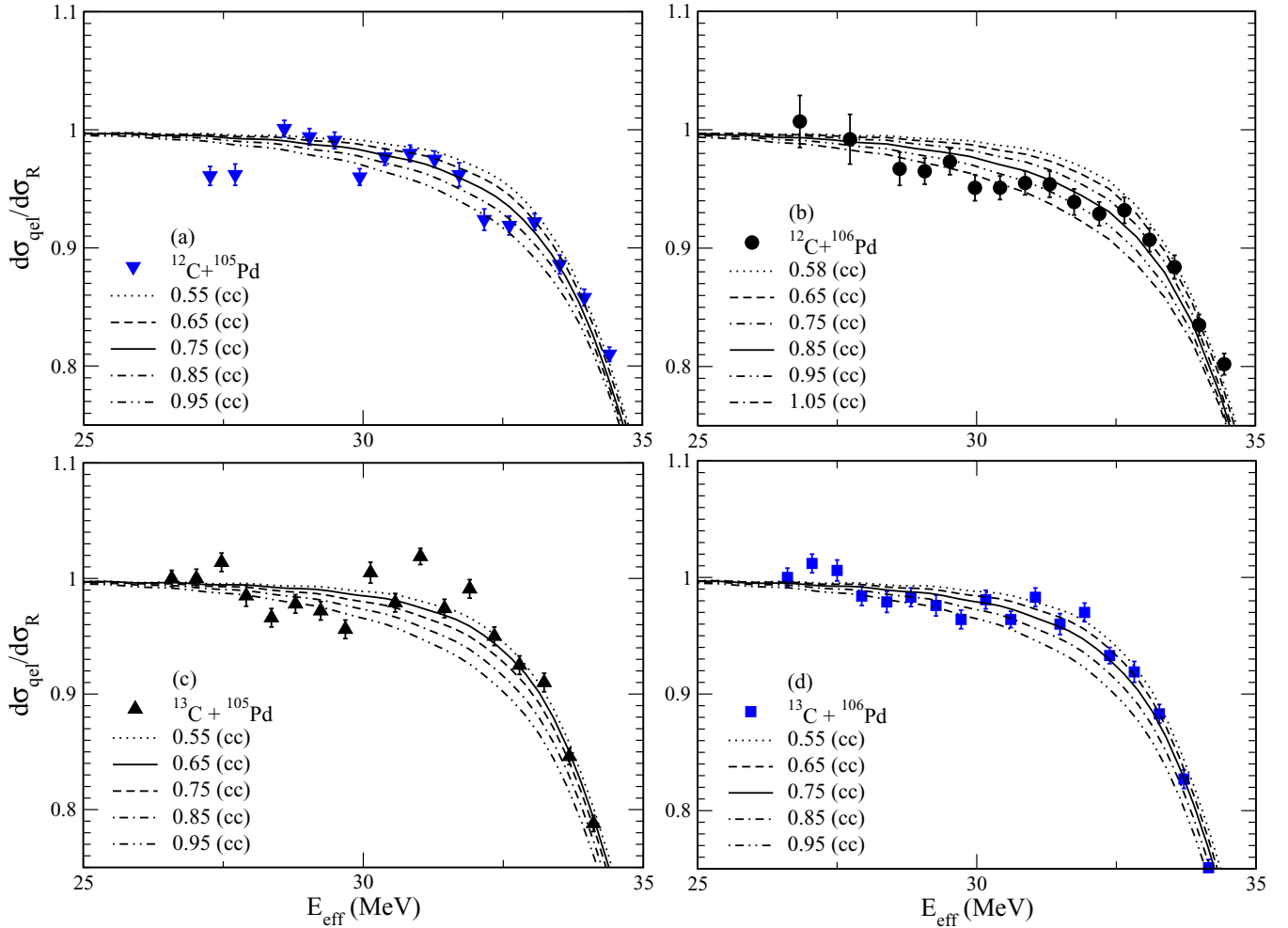


FIG. 3. (Color online) Same as Fig. 1, but with the coupled-channels calculations.

those in literature. It can be observed from the table that those nuclei which exhibit a large channel-coupling effect on surface diffuseness parameter have a small excitation energy of the first excited state, i.e.,  $E^* < 1$  MeV. In contrast, the first vibrational

TABLE III. The deformation parameter,  $\beta$ , the excitation energy,  $E^*$ , and the spin parity for the vibrational state in spherical target nuclei involved in the coupled-channel calculations. The values for the odd-mass nucleus,  $^{105}\text{Pd}$ , are estimated by averaging those quantities for the neighboring  $^{104}\text{Pd}$  and  $^{106}\text{Pd}$  nuclei. The values are taken from the references listed. The table also lists those quantities for the deformed nuclei studied in Ref. [17], that is,  $^{186}\text{W}$  and  $^{170}\text{Er}$ .

Nucleus	$\beta$	$E^*$ (MeV)	State	Ref.
$^{208}\text{Pb}$	0.111	2.615	$3^-$	[29]
$^{92}\text{Mo}$	0.140	2.849	$3^-$	[27]
$^{105}\text{Pd}$	0.219	0.534	" $2^+$ "	[20]
$^{106}\text{Pd}$	0.229	0.512	$2^+$	[20]
$^{186}\text{W}$	0.226	0.112	$2^+$	[20]
$^{170}\text{Er}$	0.336	0.0786	$2^+$	[20]

state of  $^{208}\text{Pb}$  is at 2.615 MeV, and thus the channel coupling effect is much smaller.

Evidently, it is both  $\beta$  and  $E^*$  which are responsible for the influence of channel-coupling effect on the surface diffuseness parameter. The nature of coupling scheme, that is, the rotational versus vibrational, is unimportant with respect to the influence on the diffuseness.

### C. Role of transfer coupling

In the coupled-channels calculation shown in the previous subsection, the couplings to the quadrupole vibrational states are considered. If these were the only dominant channels, one would expect that the extracted surface diffuseness parameters were similar among the systems.

Figure 4 shows the diffuseness parameter extracted with the single-channel (the open symbols) and the coupled-channels (the filled symbols) calculations as a function of the mass product of the projectile and the target nuclei,  $A_t A_p$ . It can be observed from the figure that the diffuseness parameter is reduced as the projectile isotope is changed from  $^{12}\text{C}$  to  $^{13}\text{C}$  (with the same target isotope) or the target isotope is changed

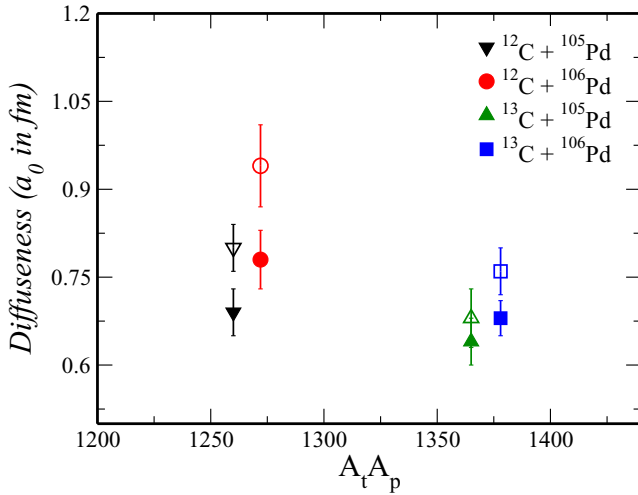


FIG. 4. (Color online) The extracted surface diffuseness parameter for the  $^{12,13}\text{C} + ^{105,106}\text{Pd}$  systems as a function of the product of masses of the projectile and target nuclei,  $A_t A_p$ . The open and filled symbols represent the results of the single-channel and the coupled-channel calculations, respectively.

from  $^{106}\text{Pd}$  to  $^{105}\text{Pd}$  (with the same projectile isotope). This gives us a hint that there could be an effect of channel coupling involved other than the collective quadrupole excitations. As we have discussed in Sec. II, the transfer channel is a promising candidate for this, since a large probability of transfer is expected for  $^{13}\text{C}$  due to the presence of the valence neutron.

In order to investigate the role of transfer couplings, we have plotted in Fig. 5 the optimum value of surface diffuseness parameter as a function of the  $Q$  value for neutron transfer. Since for the present systems, the two-neutron ( $2n$ ) transfer is a second step process, the most important transfer channel is a one-neutron ( $1n$ ) transfer, which may not be a general case. Hence, we have plotted the surface diffuseness as a function of the  $Q$  value for the  $1n$  transfer channels. For

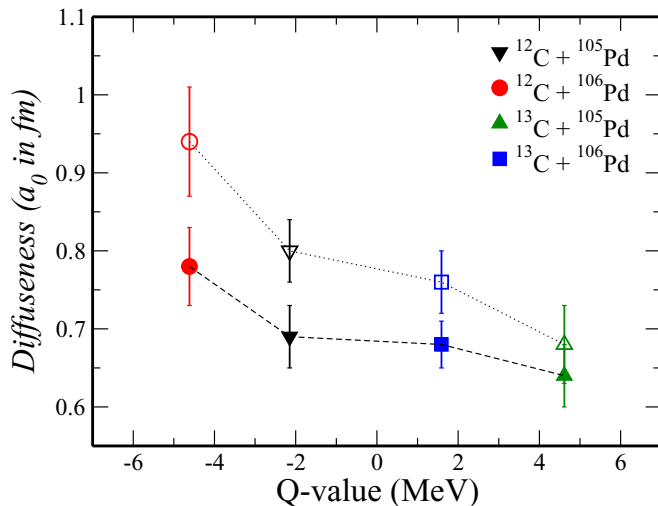


FIG. 5. (Color online) Same as Fig. 4, but as a function of the  $Q$  value for the neutron transfer channels. The lines are to guide the eye.

the  $1n$  transfer channels, we have considered the  $+1n$  and the  $-1n$  channels for the  $^{12}\text{C}$  and  $^{13}\text{C}$  projectile nuclei, respectively. These would be most preferable transfer channels from the point of view of the transfer  $Q$  value, although the  $+1n$  channel may be equally important for the  $^{13}\text{C} + ^{105}\text{Pd}$  system. It can be observed from the figure that, as a general trend, the surface diffuseness decreases as the transfer  $Q$  value increases. This might indicate that the difference in the surface diffuseness parameter between the  $^{12}\text{C}$  projectile and the  $^{13}\text{C}$  projectile could be attributed to the influence of neutron transfer coupling. It would be an intriguing future work to confirm this conjecture by carrying out coupled-channels calculations including both the collective excitations and the neutron transfer channels, although it is beyond the scope of the present paper.

#### IV. SUMMARY

The value of surface diffuseness parameter in the inter-nuclear potential for the  $^{12}\text{C} + ^{105,106}\text{Pd}$  and  $^{13}\text{C} + ^{105,106}\text{Pd}$  systems has been extracted from the measured quasielastic scattering cross sections at a backward angle. To this end, both the single-channel calculations and the coupled-channels calculations including the quadrupole vibrational excitations in the target nuclei have been carried out. Even though the systems studied involve spherical nuclei, the comparison of the coupled-channels calculations with the single-channel calculations revealed the reduction in the values of the diffuseness parameter. A similar reduction had been reported earlier for deformed systems due to the rotational coupling. Evidently, the conclusion in Refs. [17–19] that the vibrational excitation has a marginal effect on the surface diffuseness parameter is not a general one, but instead, the effect becomes significant even for the vibrational coupling when the coupling is strong enough. We have argued that the reduction in the extracted diffuseness parameter is due to the strong coupling to the low-lying collective states, and the nature of coupling is not important. That is, the reduction can be observed both for the rotational and the vibrational couplings as long as the coupling strength is large enough. Furthermore, a discussion has been made in order to understand the influence of the transfer coupling on the surface diffuseness parameter. We have observed that the surface diffuseness parameter gets smaller as the transfer  $Q$  value increases. This implies that the surface diffuseness tends to be smaller when the transfer coupling is stronger. It would be an interesting future work to confirm whether this trend holds in other systems as well. For that purpose, it would be interesting also to perform coupled-channels calculations including the transfer degree of freedom and carry out systematic studies in order to clarify the interplay between the collective excitations and the transfer couplings.

#### ACKNOWLEDGMENT

One of the authors, G.K., acknowledges the University Grants Commission (UGC), New Delhi, India for providing the financial assistance for this work.

- [1] S. G. Steadman and M. J. Rhoades-Brown, *Annu. Rev. Nucl. Part. Sci.* **36**, 649 (1986).
- [2] M. Dasgupta, D. J. Hinde, N. Rowley, and A. M. Stefanini, *Annu. Rev. Nucl. Part. Sci.* **48**, 401 (1998).
- [3] A. B. Balantekin and N. Takigawa, *Rev. Mod. Phys.* **70**, 77 (1998).
- [4] K. Hagino and N. Takigawa, *Prog. Theor. Phys.* **128**, 1061 (2012).
- [5] B. B. Back, H. Esbensen, C. L. Jiang, and K. E. Rehm, *Rev. Mod. Phys.* **86**, 317 (2014).
- [6] A. M. Stefanini, D. Ackermann, L. Corradi, J. H. He, G. Montagnoli, S. Beghini, F. Scarlassara, and G. F. Segato, *Phys. Rev. C* **52**, R1727(R) (1995).
- [7] M. Dasgupta, D. J. Hinde, J. R. Leigh, and K. Hagino, *Nucl. Phys. A* **630**, 78 (1998).
- [8] K. Hagino, M. Dasgupta, I. I. Gontchar, D. J. Hinde, C. R. Morton, and J. O. Newton, in *Proceedings of the Fourth Italy-Japan Symposium on Heavy-Ion Physics, Tokyo*, edited by K. Yoshida *et al.* (World Scientific, Singapore, 2002), p. 87.
- [9] I. I. Gontchar, D. J. Hinde, M. Dasgupta, and J. O. Newton, *Phys. Rev. C* **69**, 024610 (2004).
- [10] R. A. Broglia and A. Winther, *Heavy Ion Reactions*, Frontiers in Physics Lecture Note Series Vol. 84 (Addison-Wesley, Redwood City, CA, 1991).
- [11] M. Lozano and G. Madurga, *Nucl. Phys. A* **334**, 349 (1980).
- [12] J. O. Newton, R. D. Butt, M. Dasgupta, D. J. Hinde, I. I. Gontchar, C. R. Morton, and K. Hagino, *Phys. Lett. B* **586**, 219 (2004).
- [13] J. O. Newton, R. D. Butt, M. Dasgupta, D. J. Hinde, I. I. Gontchar, C. R. Morton, and K. Hagino, *Phys. Rev. C* **70**, 024605 (2004).
- [14] K. Hagino, T. Takehi, A. B. Balantekin, and N. Takigawa, *Phys. Rev. C* **71**, 044612 (2005).
- [15] K. Washiyama, K. Hagino, and M. Dasgupta, *Phys. Rev. C* **73**, 034607 (2006).
- [16] D. S. Monteiro, J. M. B. Shorto, J. F. P. Huiza, P. R. S. Gomes, and E. Crema, *Phys. Rev. C* **76**, 027601 (2007).
- [17] L. R. Gasques, M. Evers, D. J. Hinde, M. Dasgupta, P. R. S. Gomes, R. M. Anjos, M. L. Brown, M. D. Rodríguez, R. G. Thomas, and K. Hagino, *Phys. Rev. C* **76**, 024612 (2007).
- [18] M. Evers, M. Dasgupta, D. J. Hinde, L. R. Gasques, M. L. Brown, R. Rafiei, and R. G. Thomas, *Phys. Rev. C* **78**, 034614 (2008).
- [19] C. L. Jiang, K. E. Rehm, B. B. Back, H. Esbensen, R. V. F. Janssens, A. M. Stefanini, and G. Montagnoli, *Phys. Rev. C* **89**, 051603(R) (2014).
- [20] O. A. Capurro, J. E. Testoni, D. Abriola, D. E. DiGregorio, G. V. Martí, A. J. Pacheco, M. R. Spinella, and E. Achterberg, *Phys. Rev. C* **62**, 014613 (2000).
- [21] R. A. Broglia, C. H. Dasso, S. Landowne, and A. Winther, *Phys. Rev. C* **27**, 2433(R) (1983).
- [22] K. Hagino, N. Rowley, and A. T. Kruppa, *Comput. Phys. Commun.* **123**, 143 (1999).
- [23] R. Bass, *Phys. Rev. Lett.* **39**, 265 (1977).
- [24] K. Hagino, N. Takigawa, and S. Kuyucak, *Phys. Rev. Lett.* **79**, 2943 (1997).
- [25] H. Timmers, J. R. Leigh, M. Dasgupta, D. J. Hinde, R. C. Lemmon, J. C. Mein, C. R. Morton, J. O. Newton, and N. Rowley, *Nucl. Phys. A* **584**, 190 (1995).
- [26] K. Hagino and N. Rowley, *Phys. Rev. C* **69**, 054610 (2004).
- [27] T. Nakagawa *et al.*, *J. Nucl. Sci. Technol.* **32**, 1259 (1995).
- [28] S. Raman, C. W. Nestor, Jr., and P. Tikkanen, *At. Data Nucl. Data Tables* **78**, 1 (2001).
- [29] T. Kibédi and R. H. Spear, *At. Data Nucl. Data Tables* **80**, 35 (2002).